HYBRID ENERGY SYSTEM MODELING AND CONTROL

Milana Trifkovic[1], Mehdi Sheikhzadeh[2], Khaled Nigim[2] and Prodromos Daoutidis[1*]
1. University of Minnesota, Minneapolis, MN
2. Lambton College, Sarnia, ON, Canada

Abstract

This study deals with system integration and power management of a stand-alone renewable energy (RE) hybrid system, which is in its final stage of construction in Lambton College (Sarnia, Ontario, Canada). The system consists of five main components: photovoltaic (PV), wind turbine, electrolyzer, hydrogen storage tanks and fuel cell. The model for each process component was developed and the hybrid energy system was successfully integrated. A two level control system, including a supervisory controller which ensures the power balance between intermittent renewable energy generation and dynamic load demand, and local individual controllers for the PV, wind, electrolyzer and fuel cell units, was implemented. The hybrid system was designed and modeled in a Matlab/Simulink environment.

Keywords

Hybrid Energy System, Power Management, Model Predictive Control (MPC).

Introduction

Renewable energy sources are becoming increasingly important as a promising path for replacement of fossil fuels. Among available renewable energy technologies, wind and solar energy are the most promising options. Although these technologies are improving in various aspects, the drawbacks associated with them, such as their intermittent nature and high capital cost, remain the main obstacles for their utilization. Consequently, only 6.4% of the world's total available renewable energy sources are used today. In order to obtain a more consistent energy flow for the user demand, there has been a growing trend to combine the renewable energy sources with diesel generators, battery bank, ultra-capacitors, or hydrogen production systems (Santarelli et al., 2004). A common short-term solution for energy storage is a battery bank, which offers advantages of high efficiency and fast charge/discharge capacity but also disadvantages of low energy density, self-discharge, leakage and environmental pollution. On the other hand, hydrogen is a clean fuel with a high energy density, and can be stored for long periods without significant energy loss.

Several stand-alone power systems with different combinations of renewable energy sources and energy storage systems have been studied recently (Wang et al., 2008, Qi et al., 2010). One of the main challenges for autonomous hybrid energy systems is the design of a suitable power management system that ensures meeting the customer load demand despite the intermittent nature of the renewable energy sources. Significant research effort has been made in modeling and control of individual process components of such hybrid systems (Lopez et al., 2007, Gorgun, 2006, Vahidi et al., 2006, Zhou et al., 2008). However, limited research has focused on the control of standalone hybrid systems comprising of multiple components (Zhou et al., 2008, Wang et al., 2008, Yilanci et al., 2009).

The objective of this paper is firstly to develop a comprehensive model for the stand-alone wind/PV/ electrolyzer/fuel cell system, and secondly to design a

* To whom all correspondence should be addressed

suitable power management tool. A two level control structure, consisting of a supervisory controller and a set of local controllers, was developed. A Maximum Power Point Tracking (MPPT) on the PV system, and pitch angle and power controllers on the wind turbine ensure optimal power generation by renewable energy sources. The supervisory controller computes the power references for the fuel cell and electrolyzer subsystems at each sampling time. The power references are sent to a local decentralized model predictive control (MPC) system, which brings the fuel cell and electrolyzer subsystems to the desired power reference values while minimizing the a suitable cost function. The performance and effectiveness of the proposed control architecture is demonstrated through a representative case study.

Unit Sizing and Modeling

The sizing of the various process components was performed according to the electricity energy balance for small loads typical of residential demand. This load demand is intermittent in nature, and was assumed that its minimum, maximum and average load demand values are 0.5, 1.9 and 1 kW, respectively. The sizing was performed according to the net power, which is estimated based on the difference of the power generated by wind and PV and the power demand at all times (Wang et. al., 2008).

Assuming a capacity factor (combination of the overall unit efficiency and the effect of geographical location) of 15% and 10% for the wind turbine and PV array respectively, a 4kW rated wind power, and 1.9kW PV rated power were estimated. The fuel cell needs to supply the maximum load demand when there is no sufficient power generated by the PV and wind. Therefore, the estimated size of the fuel cell stack is 1.9kW. The electrolyzer capacity should be adequate to use the surplus power from the RE sources. The maximum excess power will occur when there is minimum load and maximum power from the renewable energy sources, which corresponds to a 5.9kW electrolyzer capacity. However, the situation when both wind and solar power reach their maximum points while the load demand is at its lowest is very unlikely, and thus a 3kW capacity for the electrolyzer was used.

The model for each process component is described in the following subsections.

Wind Conversion System

A variable-speed wind turbine with doubly fed inductance generator was implemented in the proposed system. The wind turbine consists of three main components: turbine rotor, drive train and generator.

The power extracted from wind by the turbine rotor is given by:

$$P_w = \frac{1}{2}\rho A v^3 c_p(\lambda,\beta) \tag{1}$$

where P_w is the power extracted from the wind, ρ is the air density, A is the swept area, v is the wind speed and c_p is the power coefficient which is a function of the tip speed ratio (λ) and the pitch angle of the rotor blades (β).

The drive train transfers the power from the turbine rotor to the generator. The main modeling equations for the drive train are as follows:

$$\frac{d\omega_M}{dt} = \frac{1}{2H_M}\left(T_M - K\cdot\theta_{MG} - D_M\cdot\omega_M\right) \tag{2}$$

$$T_M = \frac{P_w}{\omega_M} \tag{3}$$

where T_M is the accelerating torque, K is the effective shaft stiffness, θ_{MG} is the twist in the shaft system, ω_M is the speed of the wind turbine, and $D_M\omega_M$ is the damping torque in the wind turbine.

A Park model approach is commonly used for the induction generator simulation. The stator is directly connected to the grid and the stator voltage (v_s) is imposed by the grid. The rotor voltage (v_r) is controlled by a converter and is used to perform the machine control (Lopez et al. 2007). This model can be described as follows:

$$\vec{v}_s = R_s\cdot\vec{i}_s + \frac{d}{dt}\vec{\psi}_s \tag{4}$$

$$\vec{v}_r = R_r\cdot\vec{i}_r + \frac{d}{dt}\vec{\psi}_r - j\omega_r\vec{\psi}_r \tag{5}$$

where $\vec{i}$ is the current space vector, $\vec{\psi}_s$, $\vec{\psi}_r$ are the stator and rotor impendence, and R_s, R_r are the rotor and stator resistance.

Photovoltaic (PV) Conversion System

The PV process is a physical process through which solar energy is converted directly into electrical energy. The relationship between the output PV voltage V and the load current I of a PV cell or a module can be expressed as:

$$I_{PV} = I_{SC} - I_D - \frac{V_D}{R_P} \tag{6}$$

$$V_{PV} = V_D - R_S I_{PV} \tag{7}$$

$$I_D = I_O\left(e^{V_D/V_T} - 1\right) \tag{8}$$

where I_{SC} is the short-circuit current of the PV cell, I_0 is the saturation current, I_{PV} is the load current, V_{PV} is the PV output voltage, R_s is the series resistance of the PV cell, V_D is the diode voltage and I_D is the diode current.

In this study, the effect of temperature on the PV panel was not considered. A PV system consists of array of cells connected in series and parallel to provide the desired output terminal voltage and current.

Electrolyzer Unit

Once the power generated by the RE system is higher than the load demand, hydrogen generation by the water splitting reaction is initiated in the electrolyzer. The

dynamic model for a PEM electrolyzer is composed of four ancillaries: anode, cathode, membrane and voltage ancillary (Gorgun, 2006). The required applied voltage to the electrolyzer can be written as:

$$V_{ele} = E - V_{act} - V_{ohm} - V_{conc} \quad (9)$$

where E is the equilibrium voltage, V_{ohm} is the ohmic over-potential, V_{act} is the activation over-potential, and V_{conc} is the concentration over-potential. The equilibrium voltage can be expressed by the Nernst equation:

$$E = E_o + \frac{RT_{ele}}{2F}\left[ln\left(\frac{P_{H_2} P^{0.5}_{O_2}}{P_{H_2O}}\right)\right] \quad (10)$$

where E_0 is the standard potential, R is the universal gas constant, F is the Faraday constant, T_{ele} is the absolute temperature, and, P_{H2} , and P_{O2} are the partial pressures of water, hydrogen, and oxygen, respectively.

The activation over-potential is related to the electrode kinetics at the reaction site and is calculated according to:

$$V_{act} = \frac{2RT_{ele}}{\alpha F}\ln\left(\frac{i}{2i_0}\right) \quad (11)$$

where i_0 is the exchange current density and α is the charge transfer coefficient. The Ohmic over-potential is expressed in terms of membrane resistance:

$$V_{ohm} = iR_{ohm} \quad (12)$$

The concentration over-potential is given by:

$$V_{conc} = i\left(v_{c_1}^{conc}\frac{i}{i_{\max}}\right)^{v_{c2}^{conc}} \quad (13)$$

The material balance equations are derived on each electrode according to the following equations:

$$\frac{dN_{O_2}}{dt} = F_{O_2}^{in} - F_{O_2}^{out} + \frac{nI}{4F}\eta_F \quad (14)$$

$$\frac{dN_{H_2O}}{dt} = F_{H_2O}^{in} - F_{H_2O}^{out} \pm F_{H_2O}^{eod} \pm F_{H_2O}^{d} \quad (15)$$

$$\frac{dN_{H_2}}{dt} = F_{H_2}^{in} - F_{H_2}^{out} + \frac{nI}{2F}\eta_F \quad (16)$$

where N_{H2O}, N_{H2} , and N_{O2} are molar hold-ups of water, hydrogen, and oxygen, respectively. Note that the ± in Eq. (15) indicates that terms change sign in the water mass balance on the cathode and the electrode side. The energy balance takes the following form:

$$M_{ele}C_{ele}\frac{dT}{dt} = \dot{Q}_{gen} - \dot{Q}_{loss} - \dot{Q}_{cool} \quad (17)$$

Hydrogen Storage and Compression Unit

Hydrogen produced in the electrolyzer is compressed prior to its storage. The required power for the centrifugal compressor is calculated by the following equation:

$$P_{comp} = 2n_{H_2}^{comp,in}\left(\frac{mRT^{comp,in}}{m-1}\right)\left[\left(\frac{p^{sto,in}}{p^{comp,in}}\right)^{\frac{m-1}{m}} - 1\right]\frac{1}{\eta_{comp}} \quad (18)$$

A modified equation of state (Beattie-Bridgeman equation) was used to describe pressure in the hydrogen gas storage:

$$P^{sto} = \frac{n_{H_2}^{2sto}\,RT^{sto}}{V^{sto^2}}\left(1-\frac{cn_{H_2}^{sto}}{V^{sto}T^{sto^3}}\right)\left[\frac{V^{st}}{n_{H_2}^{sto}} + B_0\left(1-\frac{bn_{H_2}^{sto}}{V^{sto}}\right)\right] - \frac{A_0 n_{H_2}^{2sto}\left(1-\frac{an_{H_2}^{sto}}{V^{sto}}\right)}{V^{sto^2}} \quad (19)$$

where A_0, B_0, a, b, c are constants. Mass and energy balances over the hydrogen tank can be used to estimate the amount of hydrogen and temperature inside the tank.

Fuel Cell

The reverse equivalent of a PEM electrolyzer is a PEM fuel cell. The chemical energy of a hydrogen fuel is converted into electricity through a chemical reaction with oxygen. The byproducts of this chemical reaction are water and heat.

The dynamic fuel cell model used here is developed in Pukrushpan et al. (2004), and it is divided into four main ancillaries: anode, cathode flow, stack voltage, and membrane hydration. The model assumes that humidity is regulated to the desired level and does not take into account humidity fluctuations.

Similarly to the electrolyzer voltage, Eq. (9), the fuel cell voltage calculation takes into account the activation, ohmic and concentration over-potentials.

Mass balances for the anode and cathode are shown below. In comparison to the electrolyzer, the mass balance for nitrogen is present due to the fact that air is used as a source of oxygen.

$$\frac{dN_{O_2}}{dt} = F_{O_2}^{in} - F_{O_2}^{out} - \frac{nI_{fc}}{4F} \quad (20)$$

$$\frac{dN_{N_2}}{dt} = F_{N_2}^{in} - F_{N_2}^{out} \quad (21)$$

$$\frac{dN_{H_2O}}{dt} = F_{H_2O,v}^{in} - F_{H_2O,v}^{out} \pm \frac{nI_{fc}}{2F} \pm F_{H_2O,v}^{mem} \quad (22)$$

$$\frac{dN_{H_2}}{dt} = F_{H_2}^{in} - F_{H_2}^{out} - \frac{nI_{fc}}{2F} \quad (23)$$

Note that the nitrogen mass balance is only applicable on the cathode side, and the hydrogen mass balance on the anode side of the fuel cell. The energy balance is given by the following equation:

$$M_{fc}C_{fc}\frac{dT}{dt} = \dot{Q}_{chem} - \dot{Q}_{elec} - \dot{Q}_{sens+latent} - \dot{Q}_{loss} \quad (24)$$

Control Structure

The control system consists of a supervisory controller for the overall power management, and secondary low level controllers, which manage various parameters for the individual components.

Decision Based Power Management Formulation

The power flow in the hybrid system is shown in Figure 1. The converted energy from the renewable

sources can be either used directly to meet the load demand, or transferred to the hydrogen production process. The logic of the decision process is based on the following equation:

$$P_{net} = (P_{wind} + P_{pv}) - (P_{load} + P_{ae}) \quad (25)$$

where P_{load} is the load demand and P_{ae} is the power consumed by auxiliary equipment including compressors, controllers and safety equipment.

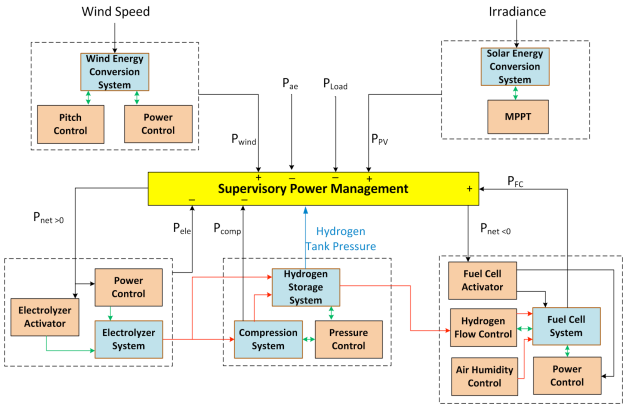

Figure 1. Power management for hybrid energy system

At each sampling interval, if the excess wind and PV generated power is greater than the rated power of the electrolyzer ($P_{net} < P_{ele}$), the electrolyzer stack is activated to generate hydrogen, which is then delivered to the hydrogen storage tanks through the compressor unit. On the other hand, when there is a deficit in power generation ($P_{net} < 0$), the FC stack is activated to consume the stored hydrogen and convert it to electricity. The fuel cell activation will occur if there is enough hydrogen in the storage tank. Otherwise, the hybrid system enters the "hydrogen starvation" mode. This can occur as a consequence of either extreme operational conditions, such as low availability of renewable energy and very high load demand, or inappropriate unit sizing. An additional problem is operating the electrolyzer and fuel cell at their full capacities, i.e. without any local control. The amount of power required to run the electrolyzer depends on its capacity, and if it is operated at the rated capacity, at some point even if $P_{net} > 0$, the amount of power consumed by the electrolysis process would overcome the power generated by the RE sources. The solution to this problem is implementation of local controllers on the electrolyzer and fuel cell. Their primary objective is to ensure using the suitable extent of the electrolyzer and fuel cell's capacity in order to use the excess energy and stored hydrogen in the most efficient way.

Local Controllers

The local, or low level, controllers ensure maximum energy extraction of the RE side of the hybrid system, as well as proper hydrogen generation and utilization.

Despite all improvements, PV modules still have relatively low conversion efficiency. *V-I* and *V-P* characteristic curves for a PV array specify a unique operating point at which the maximum possible power is delivered. The Maximum Power Point Tracking (MPPT) algorithm is used for extracting the maximum available power from the PV module under certain voltage and current conditions. There are several MPPT techniques reported in the literature. The perturbation and observation method (P&O) is one of the common and effective ways of power tracking for PV arrays (Esram and Chapman, 2007). In this study the current perturbation and observation method (CP&O) was applied. The MPP tracker operates by periodically incrementing or decrementing the solar array current. If a given perturbation leads to an increase (decrease) of the output power of the PV, then the subsequent perturbation is generated in the same (opposite) direction.

The wind turbine power output varies with the wind speed. The control objective is dependent on the wind velocity range. Above the cut-in wind speed, the control system extracts maximum power according to the turbine specific maxima power trend. The control action is based on the difference between the actual turbine speed (ω_r) and the corresponding maxima power. This offset is sent to two PID controllers to adjust the current and voltage of the rotor converter in order to obtain the maximum power. Between the rated and cut-out speed, the pitch angle controller takes action. In this velocity range, the turbine speed (ω_r) is compared to the desired turbine speed and the offset is sent to the pitch controller to manipulate the pitch angle and keep the output power constant. The pitch angle operational range and its rate of change are the constraints applied on this controller. In the case of wind speed higher than the cutout speed, the system is taken out of the operation for the protection of its components.

As previously mentioned, the electrolyzer and fuel cell are commonly operated at their maximum capacity and this can drastically decrease the overall efficiency of the system. In this study, separate model predictive controllers are designed and applied to control the electrolyzer and fuel cell performance.

For control design purposes, the nonlinear models of the electrolyzer and fuel cell were linearized around selected operating points to obtain a state space model in the following form:

$$\begin{cases} \dot{x} = Ax + Bu + B'w \\ y = Cx \end{cases} \quad (26)$$

where *x, u, w* and y are the model states, manipulated variables, disturbances and model outputs, respectively. These variables for the electrolyzer are:

$$\begin{cases} x_{ele} = [\delta N_{O_2,a},\ \delta N_{H_2O,a},\ \delta N_{H_2,c},\ \delta N_{H_2O,c}]^T \\ y_{ele} = [\delta P_{ele},\ \delta V_{ele},\ \delta N_{H_2},\ \delta p_{H_2}]^T \\ u_{ele} = [\delta I_{ele}] \\ w_{ele} = [\delta P_{ele}] \end{cases} \quad (27)$$

where the operator δ indicates the deviation from the operating point, I_{ele} is the electrolyzer's current, P_{ele} is the electrolyzer's consumed power, V_{ele} is the electrolyzer voltage, p_{ele} is the electrolyzer's operation pressure. P_{ele} is considered as the controlled variable and other outputs are measured outputs. The other parameters have been introduced in the electrolyzer modeling section.

The fuel cell state space model variables are:

$$\begin{cases} x_{fc} = [\delta p_{fc}, \delta N_{H_2,a}, \delta N_{H_2O,a}, \delta N_{N_2,c}, \delta N_{O_2,c}]^T \\ y_{fc} = [\delta P_{fc}, \delta V_{fc}]^T \\ u_{fc} = [\delta I_{fc}] \end{cases} \quad (28)$$

where P_{fc} is the fuel cell generated power, chosen as the controlled variable, and V_{fc} is fuel cell voltage, considered as the measured output.

For both systems, the control objective is to keep the power (P_{ele} and P_{fc}) at desired set-points which are imposed by the P_{net} value from the power management controller (Eq. (25)). Constraints on upper and lower limits as well as the rate of change for power were implemented to avoid large and non-realistic variations.

The model predictive controller is designed to minimize the following finite control and horizon performance index:

$$\min \sum_{i=1}^{n_y} \left\| \alpha \left[y_i - y_{i,ref} \right] \right\|^2 + \sum_{i=1}^{n_u} \left\| \beta \left[\Delta u_i \right] \right\|^2$$
$$s.t. \begin{cases} y_{lb} \le y \le y_{ub} \\ \Delta y_{lb} \le \Delta y \le \Delta y_{ub} \\ u_{lb} \le u \le u_{ub} \end{cases} \quad (29)$$

where α and β are input and output weight factors and n_y and n_u are the prediction and control horizons. The objective function was subjected to the set of constraints, the fuel cell and electrolyzer's operational limitations (y_{ub}, y_{lb}, u_{ub}, u_{lb}) and the rate of change in the electrolyzer and fuel cell power. Aside from power control, two PI controllers were implemented to minimize the pressure difference between the cathode and anode by manipulating the hydrogen flow, and keep the desired air humidity by injecting appropriate amount of water vapor into the air stream entering the cathode side of the fuel cell.

Results and Discussion

The proposed hybrid stand-alone conversion and the storage system was developed using Matlab and Simulink software. The presented simulation results are based on the average weather data for a winter day in the Sarnia, Ontario region, and the load demand for the stand-alone system built there. The generated power based on the total wind and solar energy is presented in Figure 2a, with the action of local wind and PV controllers. Figure 2b shows the total generated power, the load demand and their difference (P_{net}) power. As seen from Figure 2c, once the wind velocity is high and starts approaching the rated wind power value, the pitch controller takes the action in order to keep the turbine running at the constant rated power.

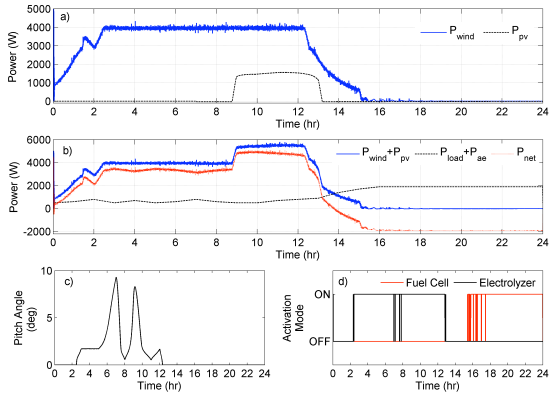

Figure 2. a) Generation, demand, and net power, b) Power generated by wind and PV, c) Pitch Angle d) FC and Electrolyzer

The P_{net} trend shown in Figure 2b is used to activate or deactivate the hydrogen system components. Figure 2d presents the electrolyzer and fuel cell status throughout the simulation period. When $P_{net} > P_{ele}$, there is an excess power available for hydrogen generation which will result in activation of the electrolyzer at its rated capacity. However in the case of $P_{net} < 0$, the total of wind and solar generated power is not adequate to meet the load demand. Under these conditions, the fuel cell is activated to supply the power shortage (see Figure 2d). It is noted that P_{net} should be less than the fuel cell rated power ($P_{net} < P_{fc}$) in order to run the fuel cell at its rated capacity.

As previously mentioned, the main objective of the power management supervisory controller is not only to enable and disable the hydrogen system components, but to manipulate them appropriately with respect to the power balance (P_{net}). The effect of additional controllers on each process component on the power consumption and conversion was simulated. The MPC was designed for the electrolyzer and fuel cell and then integrated with the nonlinear model of the plant. The length of prediction horizon affects both the computational time and performance of the system. The prediction (n_y) and control horizon (n_u) was set to 15 and 8 intervals for the electrolyzer, and 10 and 4 intervals for the fuel cell. The operational range for the electrolyzer and fuel cell are 200-3000W and 100-1900W. A variable sampling time with maximum size of 1s was implemented. The individual MPC for the electrolyzer and fuel cell was enabled when the activation signal was received from the power management controller. The remote set-point for the MPC controllers was P_{net} for the electrolyzer and $|P_{net}|$ for the fuel cell. Figures 3 and 4 show the performance of the MPC controllers implemented for the electrolyzer and fuel cell, respectively.

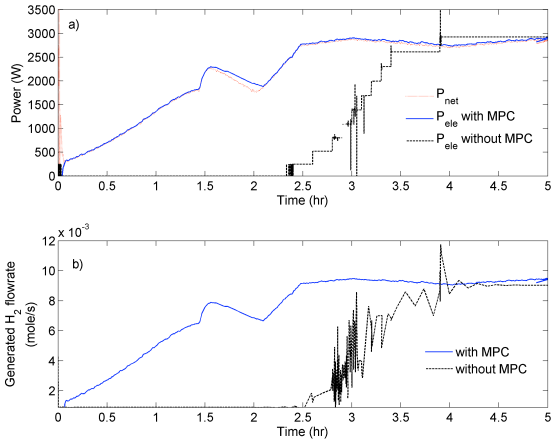

Figure 3. Electrolyzer MPC a) Performance in terms of tracking net power, b) Hydrogen generated

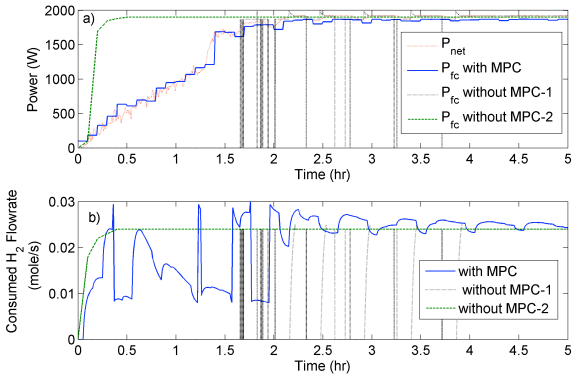

Figure 4. Fuel Cell MPC . Electrolyzer MPC a) Performance in terms of power generated, b) Hydrogen consumed

The controllers show robust set-point tracking despite all the variation in the set-points. It is important to note that the hydrogen generation by the electrolyzer and its consumption by the fuel cell are significantly more efficient. Also, note that the ability to run the electrolyzer at lower capacity enabled its activation when $P_{net}>0$ instead of $P_{net}>P_{ele}$. This in turn results in more efficient hydrogen generation as well as elimination of frequent turning on and off of the electrolyzer system. For the fuel cell, we demonstrate two criteria for the fuel cell activation without the power controller (see Figure 4). The first criterion ($P_{net} <P_{fc}$) results in the more conservative hydrogen usage, but also fails to meet the load demand. On the other hand, the second criterion ($P_{net} <0$) results in over-generating electricity as the fuel cell is always operated at its maximum capacity with previously stored hydrogen depleted rapidly. The implementation of the MPC eliminates these problems and results in the successful demand tracking and adequate hydrogen usage.

Conclusion

A comprehensive model for a stand-alone hybrid energy system was developed. A supervisory controller, which ensured proper power management, as well as a set of local controllers, which ensured efficient hydrogen generation and consumption were implemented. A model predictive controller was designed for optimal utilization of the electrolyzer and fuel cell. The controller performance showed significant improvement in the utilization of both components, and consequently better power management of the hybrid energy system in comparison to the case when no MPC controller was implemented.

Acknowledgements

The authors would like to acknowledge Natural Sciences and Engineering Research Canada (NSERC), which provided financial support for this project.

References

Esram, T., Chapman, P.L. (2007). Comparison of Photovoltaic Array Maximum Power Point Tracking Techniques. *IEEE Transactions on Energy Conversion* 22 (2), 439-449.

Gorgun, H. (2006). Dynamic modelling of a proton exchange membrane (PEM) electrolyzer. *International Journal of Hydrogen Energy*, 31(1), 29-38.

Lopez, J., Sanchis, P., Roboam, X., Marroyo, L. (2007). Dynamic Behavior of the Doubly Fed Induction Generator During Three-Phase Voltage Dips. *IEEE Transactions on Energy Conversion*, *22*(3), 709-717.

Qi, W., Liu, J., Christofides, P. D. (2011). Supervisory Predictive Control for Long-Term Scheduling of an Integrated Wind/Solar Energy Generation and Water Desalination System. *IEEE Trans. Contr. Syst. Techn.*, in press.

Pukrushpan, J.T., Stefanopoulou, A. G., Peng, H. (2004). Control of Fuel Cell Power Systems: Principles, Modeling, Analysis and Feedback Design. *Springer*, 1st edition. London, UK.

Santarelli, M., Cali, M., Macagno, S. (2004). Design and analysis of stand-alone hydrogen energy systems with different renewable sources. *International Journal of Hydrogen Energy*, 29(15), 1571-1586.

Vahidi, A., Stefanopoulou, A., Peng, H. (2006). Current Management in a Hybrid Fuel Cell Power System: A Model-Predictive Control Approach. *IEEE Transactions on Control Systems Technology*, 14(6), 1047-1057.

Wang, C., Member, S., Nehrir, M. H. (2008). Power management of a stand-alone wind/photovoltaic/fuel-cell energy system. *IEEE Power and Energy Society General Meeting*, 23(3), 1-10.

Zhou, K., Ferreira, J.A., de Haan, S.W.H. (2008). Optimal energy management strategy and system sizing method for stand-alone photovoltaic-hydrogen *systems International of Journal of Hydrogen Energy*, 33, 477–489.

Yilanci, a, Dincer, I., Ozturk, H. K. (2009). A review on solar-hydrogen/fuel cell hybrid energy systems for stationary applications. *Progress in Energy and Combustion Science*, 35, 231–244.